

Microbolometer for high-end commercial and defense applications in 12 μm pitch

C.G.Jakobson*, U.Mizrahi, N.Ben Ari, N.Shiloah, E.Avnon, D.Seref, G. Zohar,
R.Raichman, T.Markovitz

SCD Semiconductor Devices – P.O. Box 2250, Haifa, 31021, Israel

**Corresponding author: claudio@scd.co.il*

Abstract

This work focuses on a novel 12 μm pitch, 640x512 VGA-format uncooled microbolometer targeted at commercial and defense applications. The microbolometer is fabricated by post-processing on top of a silicon readout integrated circuit. The sensitive material used is Vanadium oxide, which is evaporated on the bolometer surface during the post-processing steps. The final product is encapsulated by Wafer-Level packaging and operates without temperature stabilization from -40 °C to 71 °C.

The microbolometer achieves 50mK NETD with a thermal time constant lower than 7msec providing an excellent figure of merit. The readout mode is based on a current-mode front end using thermally-shorted and mirror microbolometers that can be calibrated to overcome process fabrication non-uniformities.

Keywords: microbolometers, LWIR, uncooled, infrared, sensors, imaging.

I. INTRODUCTION

Micro-bolometers (μ -Bolometer) are a type of infrared sensors that are sensitive to the Long Wave Infrared (LWIR) spectrum. Microbolometer Focal Plane Arrays (FPA) are particularly of interest in thermal imaging because they can provide uncooled sensitivity at room-temperature to thermally emitted wavelengths.

Since the introduction of BIRD384 in 2005, SCD has been developing μ -Bolometers for about 2 decades starting with the 25 μm pitch products and followed by the 17 μm pitch products [1-4]. This paper focuses on a novel high-end 12 μm pitch, 640x512 VGA μ -Bolometer. This μ -Bolometer achieves 50mK Noise Equivalent Temperature Difference (NETD) with a thermal time constant lower than 7msec providing an excellent Figure of Merit (FOM).

The Readout Integrated Circuit (ROIC) supports rolling shutter integration mode up to 120Hz with

13bit ADC output. The communication to the system is done by an SPI interface that enables to control imaging features like row direction, inverse image or windowing. The overall nominal operation power for the VGA μ -Bolometer matrix and other ROIC features is 300mW and may go up to 550mW depending upon the frame rate and operation mode.

Due to their uncooled operation and their low Size Weight and Power (SWaP) the applications of μ -Bolometers are varied. In defense, security and surveillance applications the μ -Bolometers can be used to detect the presence of humans, vehicles, missiles and other possible threats characterized by their emitted heat radiation. Due to their sensitivity in the LWIR spectrum μ -Bolometers imaging can operate in no light, low light or foggy conditions. Other applications include automotive, industrial process inspection, agriculture and health care. SCD μ -Bolometers are targeted at defense and commercial applications requiring a high FOM.

II. μ BOLOMETER TECHNOLOGY

The principle of operation of the μ -Bolometer is based on small temperature changes induced by the absorption of infrared radiation leading to significant variations in its resistance. The resistance variations in the μ -Bolometers generate an electrical signal that is sensed at the ROIC, followed by its analog-to-digital conversion and the posteriorly generated video output. The leading sensitive material for μ -Bolometers today are Vanadium Oxide (VOx) and amorphous Silicon (a-Si) [5-6], selected by their high thermal sensitivity. VOx is the sensitive material at main focus at SCD.

The μ -Bolometer is fabricated by post-processing micro-machining on top of a 0.18 μm CMOS ROIC. The legs and its sensing platform are depicted in Fig. 1. The VOx is evaporated on the bolometer surface during the post-processing steps

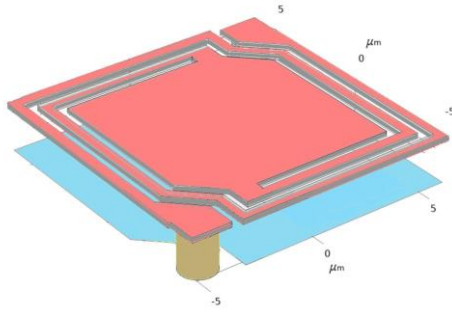


Fig. 1. μ -Bolometer

The μ -Bolometer is sensitive between the 7.5-14 μ m LWIR wavelengths, its spectral response is shown in Fig. 2. The final product is encapsulated by Wafer-Level Packaging (WLP) and operates TEC-less from -40 $^{\circ}$ C to 71 $^{\circ}$ C.

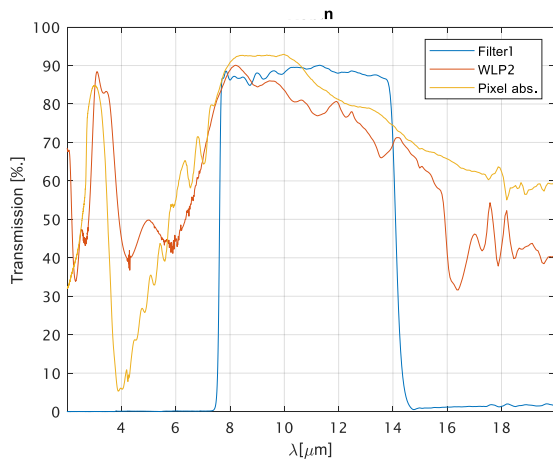


Fig. 2. μ -Bolometer Spectral Response

III. ROIC

The ROIC readout mode is based on a current-mode front end [6-10] using Thermally-Shorted (TS) and sensing μ -Bolometers. The ROIC signal path is shown in Fig. 3. The current-mode signal operation is based on the integration of the current difference between the thermally-variable μ -Bolometer and the thermally-independent μ -Bolometer. This integration is actively performed by a column parallel Charge TransImpedance Amplifier (CTIA) [6-7,9-10] that can provide adjustable gain.

A block diagram of the ROIC is shown in Fig. 4. A novel feature in this μ -Bolometer ROIC is to provide integrated frame memory for frame averaging up to 2 frames. The pixel bolometer and pixel memory are implemented pixel-wise while the column CTIA and ADC are column parallel. Following the CTIA the signal is converted by a

column parallel slope ADC and posteriorly multiplexed into the video output

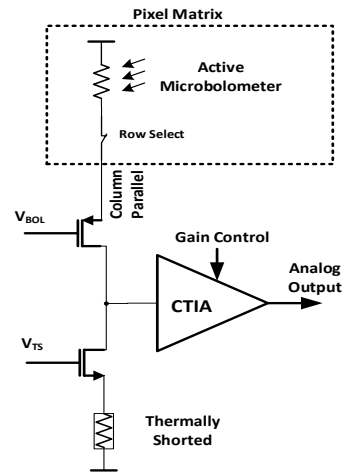


Fig. 3. ROIC Signal Path

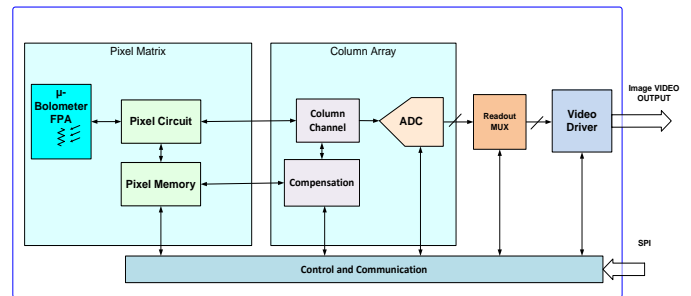


Fig. 4. ROIC Block Diagram

A requirement for TEC-less operations is to correct the non-uniformities introduced by process fabrication. These variations usually generate resistance differences larger than those generated by the sensing process. As shown in Fig. 4, a compensation mechanism is implemented at the channel level. The implementation of this non-uniformity compensation at the ROIC together with a proper design of low frequency noise enable the shutter-less operation of the μ -Bolometer for relatively long periods of time.

A wide target thermal Dynamic Range (DR) is covered from -50 $^{\circ}$ C to 150 $^{\circ}$ C. The gain of the CTIA and the integration time can be controlled to adjust to variable thermal DR. In addition, with a dedicated gain setting, the input DR can be enhanced up to a 1400 $^{\circ}$ C span.

The video output is LVCMOS using 14 bit in parallel, with an output data frequency \sim 50MHz at maximum frame rate. The nominal ADC row conversion is 32 μ sec. For fast frame rate, 8 μ sec ADC conversion time can be achieved with

reduced resolution and increased power. The ADC can be run in two modes:

- 1) Integration-Then-Read where the ADC conversion does not happen during signal integration
- 2) Integration-While-Read where the ADC conversion is simultaneous to the integration and ping-pong capacitors are used for the implementation of the ADC.

In addition, as shown in Fig. 5, the ADC can be operated in two modes, a first mode where the ADC conversion is followed by the next sample track and hold, and a second mode where the ADC conversion of a first sample is simultaneous to the track and hold of a second sample.

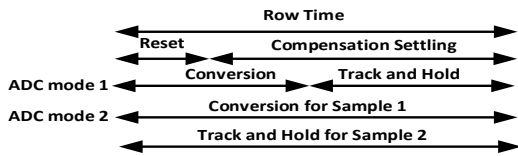


Fig. 5. ADC Timing Modes

Table 1. summarizes the μ -Bolometer array and ROIC parameters. The sensor package and ROIC prototype photo are shown in Fig. 6.

Technology	VOx Microbolometer
Format	640 x 512
Pitch	12 μ m
Temporal NETD @25C, F#1, 60Hz, 7.5 - 14 μ m	< 50mK
Thermal Time Constant	< 7 msec
Operability	> 99.5%
Frame Rate	25, 30, 50, 60, 120 Hz
Video Output	Digital, 14bit LVCMOS
Communication	SPI, QSPI
Power Dissipation @30Hz, 25C	\leq 300 mW
Package	Wafer Level Package
Size	21x21X9.5 mm2
Weight	\leq 5 g
Operation Temperature	-40°C to +71°C
FPA Temperature Stabilization	TEC-less

Table I. ROIC main imaging parameters

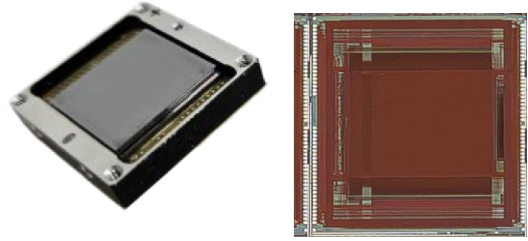


Fig. 6. Packaged sensor and ROIC Prototype Photo

IV. MEASUREMENTS

The noise level of the μ -Bolometer is targeted at \sim 2 digital levels, each digital level corresponding to \sim 25mK in nominal conditions. Fig. 7 shows the measured noise level vs. substrate variations. At nominal conditions this noise corresponds to the targeted NETD value of 50mK.

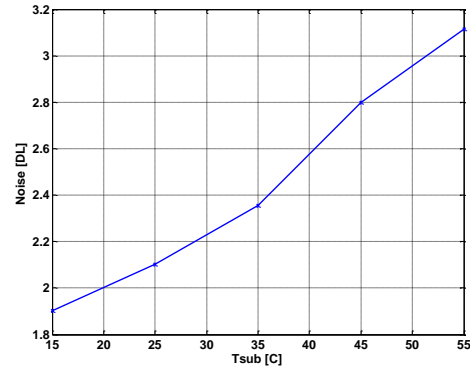


Fig. 7. Noise vs. Substrate Temperature

Fig. 8 shows the responsivity variation and signal histogram vs. the variation on the ROIC substrate temperature. The increase of the standard deviation vs. a substrate temperature increase behaves as expected.

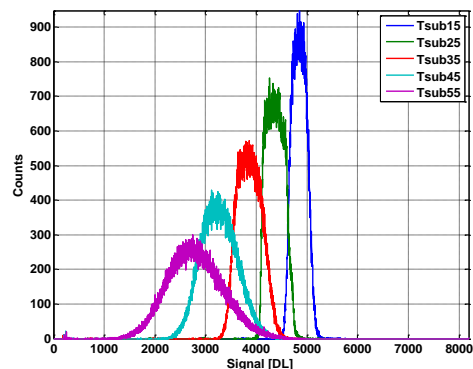


Fig. 8. Signal Hystogram vs. Substrate Temperature

Fig 9 shows the noise measured vs. the integration times for several values of the CTIA integration capacitor that controls the gain. The measured

values compared to simulation are in good agreement.

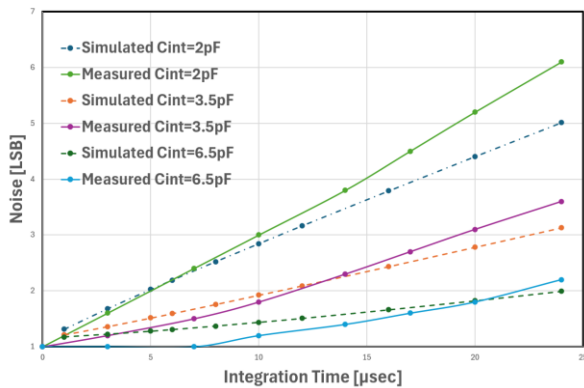


Fig. 9 Performance vs. Integration Time

Fig. 10 shows the behavior of the signal histogram response vs. gain for several values of the integration capacitor including signal noise (upper graph) and for readout noise only (lower graph)

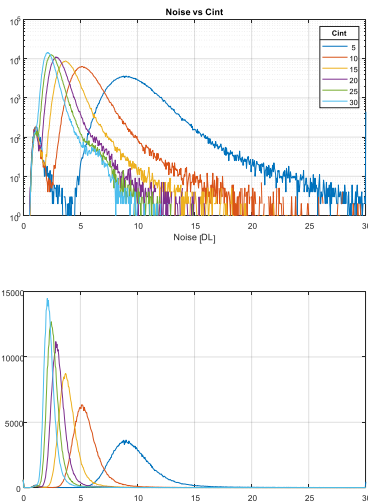


Fig. 10 Noise and Histogram vs. Integration Time

Fig. 11 shows an image capture of a construction site at daylight conditions showing a worker and the construction assembly.

V. SUMMARY

A novel 12 μm pitch VGA uncooled $\mu\text{-Bolometer}$ has been presented. Fabrication technology, ROIC architecture and main features and first measurement have been described. The $\mu\text{-Bolometer}$ is VOx based providing an NETD below 50mK and a high-end FOM. It is encapsulated by Wafer-Level Packaging and operates TEC-less from $-40\text{ }^\circ\text{C}$ to $71\text{ }^\circ\text{C}$. The first measurements of this $\mu\text{-Bolometer}$ show good results for noise, time stability, uniformity and gain behavior.



Fig. 11. Worker at construction site captured by the 12 μm $\mu\text{-Bolometer}$

VI. ACKNOWLEDGMENTS

We are in debt to a large group of engineers and technicians who conducted this work. Their dedicated work and contribution to the development and production of the detectors is highly appreciated.

VII. REFERENCES

- [1] R. Fraenkel et al. "VOx - Based Uncooled Microbolometric Detectors: Recent Developments at SCD", Infrared Technology and Applications XXXII, Proc. of SPIE Vol. 6206, 2006
- [2] R. Fraenkel et al. "SCD's Uncooled Detectors and Video Engines for a Wide Range of Applications", Infrared Technology and Applications XXXVII, Proc. of SPIE Vol. 8012, 2011.
- [3] P. Klipstein, U. Mizrahi, R. Fraenkel, I. Shritchman, "Status of Cooled and Uncooled Infrared Detectors at SCD", Defence Science Journal, Vol. 63, No. 6, pp. 555-570, 2013
- [4] R. Fraenkel et al. "Cooled and uncooled infrared detectors for missile seekers", Infrared Technology and Applications XL, Proc. of SPIE Vol. 9070, 2014
- [5] Yadav et al. "Advancements of uncooled infrared microbolometer materials: A review", Sensors and Actuators A: Physical, Vol. 342, 2022
- [6] Fusetto et al. "Readout IC Architectures and Strategies for Uncooled Micro-Bolometers Infrared Focal Plane Arrays: A Review", Journal of Sensors, mdp1, 2023
- [7] Lv et al. "Uncooled Microbolometer Infrared Focal Plane Array Without Substrate Temperature Stabilization", IEEE Sensors Journal, Vol. 14, No. 5, 2014
- [8] Liu et al. "Low-noise readout circuit for thermoelectrical cooler-less uncooled microbolometer infrared imager", Electronic Letters, Vol. 52, 2016
- [9] Hwang, S.J. et al, "A CMOS Readout IC Design for Uncooled Infrared Bolometer Image Sensors", IEEE International Symposium on Industrial Electronics, Volume 4, pp. 2788-2791, 2006
- [10] Seo et al, "An Analog Front-End IC Design for 320×240 Microbolometer Array Applications", IEEE Trans. On Circuit and Syst. Express Briefs, Vol. 62, pp. 1048-1052, 2015.